

Network Analysis and Transcriptome Profiling Identify Autophagic and Mitochondrial Dysfunctions in SARS-CoV-2 Infection

Komudi Singh¹, Yun-Ching Chen¹, Jennifer T Judy¹, Fayaz Seifuddin¹, Ilker Tunc¹, and Mehdi Pirooznia^{1,*}

Affiliations: ¹Bioinformatics and Computational Biology Laboratory, National Heart Lung and Blood Institute, National Institutes of Health, Bethesda, MD 20892, USA.

*Correspondence: Mehdi Pirooznia, mehdi.pirooznia@nih.gov

Keywords: COVID-19, SARS-CoV-2, transcriptomics, co-expression network analysis, inflammation

Abstract

Lack of effective treatment strategy and vaccine makes SARS-CoV-2 infection a big threat to mankind. Analyzing the host transcriptional changes in response to virus infection will help delineate the biological processes impacted by the virus and will potentially facilitate drug development. Using RNA seq datasets of virus infected lung cell lines A549 (infected with either SARS-CoV-2 or Influenza A virus (IAV)) and Calu3 (infected with either SARS-CoV-2 or MERS-CoV), we present a detailed analysis of genes expression changes in response to each of these viral infections. Upregulation of the antiviral interferon signaling was observed with all three viral infections. However, upregulation of the cytokine/inflammatory processes, downregulation of mitochondrial organization and respiration processes, and perturbation in the autophagic processes were specifically observed in SARS-CoV-2 infected cells, which were absent in IAV infected cells. Upregulation of the inflammatory processes was concordant with the gene expression signature of COVID-19 lungs and with inflammatory symptoms observed in severe cases of COVID-19 patients. Coexpression networks analysis also facilitated the identification of protein-protein interaction (PPI) subnetworks of genes in the inflammation and mitochondrial processes that were either coordinately up or downregulated in SARS-CoV-2 infected cells, respectively. Comparing the expression of marker genes of lung cell types from single cell RNA seq data with expression profile of A549 cells revealed that they likely represent the lung epithelial lineage cells. The cellular processes uniquely perturbed in infected cells that were identified in this analysis likely delineates lung epithelial cells response to the SARS-CoV-2 infection.

INTRODUCTION

Epidemiology

Severe Acute Respiratory Syndrome Coronavirus 2 (SARS-CoV-2) is the virus that causes the current global pandemic, coronavirus disease (COVID-19). COVID-19 presents as a wide range of clinical manifestations, ranging from asymptomatic to respiratory failure or multiorgan and systemic manifestations (1). The viral pneumonia outbreak caused by SARS-CoV-2 was first identified in Wuhan, China in December 2019. Since then, the virus has continued to spread globally, with a current transmissibility estimate (R_0) between 3-4 (2, 3). According to the World Health Organization (4) as of late April 2020, there have been over 2.8 million confirmed cases and more than 196,000 confirmed deaths across 213 countries/areas/territories. No treatments currently exist, and management strategies include supportive medical care for existing cases and social distancing for prevention. Understanding this novel pathogen and the host response it elicits is crucial to combatting the emerging threat to public health.

Human Coronavirus (hCoV) Phylogeny

SARS-CoV-2 is the 7th and most recent addition to human coronaviruses (hCoVs), which include four globally endemic hCoVs that cause a substantial portion of upper respiratory infections (229E, OC43, HKU1, and NL63), as well as two other highly pathogenic strains that have also caused recent pandemics (SARS-CoV and MERS-CoV (2, 5) in 2002-2003 and 2012, respectively (6)). All seven hCoVs are single-stranded, positive-sense RNA viruses. They all have zoonotic origins, with bats as the evolutionary reservoir host of five (229E, NL63, SARS-CoV, MERS-CoV, and SARS-CoV-2). In some cases, there are intermediate and amplifying host species as well (2). Although SARS-CoV-2 is phylogenetically similar to both MERS-CoV, and SARS-CoV (7), there are biological differences. Notably, although SARS-CoV-2 has a lower, but yet undetermined mortality rate, it is distinctly more contagious than these other highly pathogenic hCoVs, causing vastly different epidemiological dynamics. In fact, MERS-CoV was largely propagated by camel-to-human transmissions, as the virus was never able to fully adapt to optimal human-to-human transmission (8).

Pathogenicity

As obligate parasites, the viruses, while evading the host cell immune response, should encode enough proteins to ensure replication, and spread, by relying on the host cell's machinery. These processes require an intricate series of interaction between the virus and host (9). While many of the elicited responses are common across pathogens, each virus also creates a unique transcriptional profile (10). Functional distinctions across viruses may arise due to distinct processes utilized by a virus for cellular entry, or for host immune system evasion, or for replication and dissemination (11). Severity of illness for SARS-CoV-2 infections is likely impacted by both the direct cytotoxic effects of the virus, and the effectiveness of the complex host response (12, 13). While the immune response is essential to resolving the infection, dysregulation of the immune system can result in immunopathogenesis (14, 15). A dysregulated immune response is caused by rapid viral replication, cytokine storms delayed interferon response, and macrophage infiltration and excessive proinflammatory cytokines (14). This immunopathogenesis mechanism is supported by the observation of decreased viral loads occurring with increased disease severity (6). However, efforts to understand the molecular mechanisms require further study, as the unusually high morbidity and mortality of hCoVs remain unclear.

Cell/Tissue Tropism of SARS-CoV-2

The hCoVs differentially infect the human respiratory tract. The low pathogenic hCoVs infect the upper respiratory tract, and the highly pathogenic hCoVs infect the lower respiratory tract (14). Consistent with this, SARS-CoV, SARS-CoV-2, and MERS-CoV were shown to differentially infect the lung alveolar cell subtypes in cynomolgus macaques (16) and SARS-CoV elicited distinct immune response in different tissues (17). Furthermore, cell tropism study of the SARS-CoV and SARS-CoV-2 in different cell type cultures could partially explain the symptomatic differences of these two virus infections (18). Single cell (sc) transcriptomic data of the COVID-19 lung tissue have been analyzed to identify the subset of cells most prone to the SARS-CoV-2 infection and the marker genes associated with the infected cells. One such study intriguingly identified upregulation of the receptor-angiotensin-converting enzyme 2 (ACE2) in the SARS-CoV-2 infected type II pneumocyte population of the lung cells as a potential mechanism facilitating virus infection (19). Another study utilized the ACE2 and TMPRSS2

expression information at the single cell level to rank the cells based on their susceptibility to the SARS-CoV-2 infection (20). Consistent with the sc RNA seq data, dual inhibition of the host cell cysteine and serine proteases impeded viral entry into the cell (21). The cell type specific genes identified from the sc RNA seq data of COVID-19 lung samples can be further analyzed by incorporating the bulk RNA seq data to potentially identify the marker genes in COVID-19 lungs.

Here, we have analyzed the gene expression changes in A549 and Calu3 lung cell lines in response to infection with SARS-CoV-2 to identify biological processes specifically impacted by this novel coronavirus. Understanding the unique signature of SARS-CoV-2 host responses is crucial to identifying potential targets for both treatment and symptom management. We find that SARS-CoV-2 infection elicits a differential gene expression response that is unique to coronavirus infection, which is not observed in influenza A virus (IAV) infection. The differentially expressed (DE) genes that were either up or downregulated in the SARS-CoV-2 infected cells enriched in the cytokine signaling/inflammation processes, or mitochondrial processes, respectively. Additionally, the autophagic processes were also impacted in the SARS-CoV-2 infected cells. It is likely that perturbation of the mitochondrial function and autophagy could negatively impact the host cells' immune response against the viral infection leading to systemic inflammation. Furthermore, the gene expression profile of A549 cell line strongly correlated with the lung epithelial lineage cells namely the basal and ionocyte cell types from the lung single cell (sc) RNA seq data. Therefore, the biological processes identified in this study is likely representative of lung epithelial cells response to SARS-CoV-2 infection.

RESULTS

Interferon autophagy, and mitochondrial processes are impacted in cells infected with SARS-CoV-2

SARS-CoV-2 (high viral titer) vs Mock

Comparisons of gene expression profile of mock and SARS-CoV-2 infected A549 lung epithelial cell line with a higher viral titer of SARS-CoV-2 (see methods) identified >8000 DE genes. The volcano plot profiles both up-regulated and down-regulated genes in the SARS-CoV-2 infected cells (Supp Fig S1A, <https://doi.org/10.6084/m9.figshare.12272351> [Table S3]).

Pathway enrichment analysis of the DE genes showed enrichment in a wide range of biological processes (Supp Fig S1B, <https://doi.org/10.6084/m9.figshare.12272351> [Table S4]). These DE genes were classified into upregulated or downregulated following SARS-CoV-2 infection and analyzed by pathway enrichment analysis. Upregulated DE genes annotated to a wide range of pathways, notably including the interferon signaling, NFkB/cytokine signaling processes, and proteasomal degradation (Fig 1A, <https://doi.org/10.6084/m9.figshare.12272351> [Table S4]). Heatmaps highlight the upregulation of genes in cytokine, and interferon pathways, and perturbation of autophagy pathways (Fig 1B,1C,1D respectively). DE genes downregulated in the SARS-CoV-2 infected cells annotated to pathways primarily involving cell cycle and mitochondrial processes (Fig 1E, <https://doi.org/10.6084/m9.figshare.12272351> [Table S4]). A heatmap shows that the expression of the genes in mitochondria-related processes, electron transport chain and respiration were mostly downregulated in SARS-CoV-2 infected cells (Fig 1F).

SARS-CoV-2: Low viral titer vs high viral titer

Differential gene expression analysis of A549 cells infected with mock and a 10-fold lower viral titer of SARS-CoV-2 (see methods) was also performed. The resulting DE genes could be compared to the DE genes from mock vs. SARS-CoV-2 infection at higher viral titer (Fig 1). Given the exposure of cells to a lower viral titer, the number of DE genes from this comparison was smaller (196 genes) vs. the comparison of high titer SARS-CoV-2 against mock (>8000 genes) (Supp Fig S1C, <https://doi.org/10.6084/m9.figshare.12272351> [Table S3]). Analysis of the 196 DE genes showed significant enrichment in interferon and anti-viral response processes (Supp Fig S1D, <https://doi.org/10.6084/m9.figshare.12272351> [Table S4]). A pathway summary map comparing the pathway enrichment results of mock vs. high titer SARS-CoV-2 infected cells and the mock vs. low virus titer infected cells confirmed that perturbation in autophagy, inflammation, and mitochondrial processes were exclusively enriched by DE genes from the mock vs. SARS-CoV-2 infected at higher virus titer comparison (Fig 1G). SARS-CoV-2 infection at lower titer elicited robust activation of anti-viral pathways, which would likely result in recovery from the infection in a patient. Since these observations were made in a lung cell line, the concordance of the A549 cells gene expression with marker genes from different lung cell types from sc RNA seq data were calculated. Notably, the A549 gene expression was

highly correlated with the marker genes of the basal and ionocyte lung epithelial lineage cells (22, 23) (see methods, Supp Fig S7A). It is likely that the biological processes impacted in a SARS-CoV-2 infected A549 cells is likely impacted in the SARS-CoV-2 infected lung epithelial cells too. However, given the limitations of analyzing lung cell-lines data, gene expression analysis of lung samples from patient with severe or mild COVID-19 will help test if these processes are differently impacted depending on the severity of the disease. Together, these results support that SARS-CoV-2 infection impacts the expression of genes involved in the cytokine signaling, autophagy and mitochondria/respiration.

ACE2 overexpression (oe) exaggerates the gene expression fold change of a subset of genes impacted by SARS-CoV-2 infection

Mock vs. SARS-CoV-2 in ACE2 oe cells

Angiotensin-converting enzyme 2 (ACE2) is the putative primary receptor for cell entry of the SARS-CoV-2 virus (24, 25) (as well as for SARS-CoV and NL63) (26). Therefore, the gene expression profiles of ACE2 oe A549 cells infected with SARS-CoV-2 at low viral titer cells vs. mock were analyzed. The DE analysis of mock vs. low-titer SARS-CoV-2 in ACE2 oe cells identified changes in expression of a wide number of genes (Supp Fig S2A, <https://doi.org/10.6084/m9.figshare.12272351> [Table S3]). The DE gene mostly annotated to the protein trafficking, immunity, reactive oxygen species (ROS), and IL1 signaling (Supp Fig S2B). However, the DE gene list from this comparison (mock vs low-titer SARS-CoV-2 in ACE2 oe cells) showed only a small overlap with the DE gene list from the mock vs. low-titer SARS-CoV-2 comparison in A549 cells (86/4,480 DE genes; Supp Fig S2C). It is likely that the ACE2 oe facilitates viral entry and would mimic a severe virus infection state (i.e. SARS-CoV-2 infection at higher viral titer). Consistent with this, we found approximately two-thirds (2,648) of the DE genes from this mock vs. low-titer SARS-CoV-2 comparison in ACE2 oe cells overlapped with the DE genes from the previous mock vs. high-titer SARS-CoV-2 (no ACE2 oe) (Fig 2A). Of these, about half of them (1,185 genes) were upregulated in the high-titer SARS-CoV-2 infected cells. Of these 899/1,185 genes were upregulated with greater magnitude of fold changes in SARS-CoV-2 infected ACE2 oe cells (Fig 2A). About a quarter of the common DE genes were downregulated in infected cells and 50% (336/669) of these genes were further downregulated in SARS-CoV-2 infected ACE2 oe cells (Fig 2A). The remaining ~30%

(794/2648) of the common DE genes were discordantly regulated in infected cells with ACE2 oe. Partial DE genes overlap, and discordantly regulated genes are likely due to the impact of ACE2 oe on other cellular processes independent of the viral infection, or due to the effects of cell transfection protocol used to generate ACE2 oe cells.

To assess how ACE2 oe impacts the SARS-CoV-2 infection processes, pathway enrichment analysis was performed on the subset of DE genes from the high-titer comparison that were concordantly either further upregulated or downregulated in ACE2 oe infected cells. This subset analysis again implicated upregulated genes to pathways involved in inflammation, cytokine, and immunity related processes (Fig 2B, <https://doi.org/10.6084/m9.figshare.12272351> [Table S4]). The common DE genes that were further downregulated in ACE2 oe infected cells enriched in mitochondrial and respiration related processes (Fig 2C, <https://doi.org/10.6084/m9.figshare.12272351> [Table S4]). These results are consistent with the pathway enrichment results from mock vs. high-titer SARS-CoV-2 infected A549 cells (Fig 1). These results suggest that ACE2 oe exacerbates the expression profiles of a subset of genes involved in immunity, inflammation, and mitochondrial processes in A549 cells infected with SARS-CoV-2 at low viral titer. Perturbation of immunity, inflammation, and mitochondrial processes is likely indicative of a severe SARS-CoV-2 infection state.

Network analysis identified protein-protein interaction subnetworks of genes involved in interferon, inflammation and mitochondrial translation

SARS-CoV-2 vs Mock: network analysis

To further understand the potential biological processes in play during SARS-CoV-2 infection, we performed a consensus weighted gene coexpression network analysis (WGCNA) (27) on combined mock and SARS-CoV-2 infected at low and high titer cells, which identifies correlated gene clusters/modules. The WGCNA analysis identified more than 50 coexpression modules and the overlap of genes in each of these modules with significant DE genes from mock vs. SARS-CoV-2 infected at high titer is presented in the cluster dendrogram where each correlated module is represented by a color and their overlap with DE genes is shown in horizontal bars (Fig 3A, Supp Table 1).

First, pathway enrichment analysis of the correlated DE genes in the turquoise modules showed significant annotation to the mitochondria, immunity, and mRNA/transcription processes

(Fig 3B, <https://doi.org/10.6084/m9.figshare.12272351> [Table S4]). Using the GeneMANIA (28) database, protein-protein interaction (PPI) subnetworks for the DE genes in this module/cluster were identified. This analysis identified two PPI subnetworks of genes involved in interferon signaling (Fig 3C) and mitochondrial translation (Fig 3D). After incorporating the gene expression fold change information, we concluded that the interferon signaling genes were upregulated and mitochondrial genes were downregulated in SARS-CoV-2 infected cells.

Next, pathway enrichment analysis of DE genes from the blue module revealed significant annotation to unfolded protein response (UPR) and apoptosis processes (Fig 3E, <https://doi.org/10.6084/m9.figshare.12272351> [Table S4]). Using GeneMANIA database, a PPI subnetwork of genes involved in inflammation that were mostly upregulated in SARS-CoV-2 infected cells was also identified (Fig 3F). The DE genes in the brown module significantly enriched to intracellular trafficking related processes (Supp Fig S3A, <https://doi.org/10.6084/m9.figshare.12272351> [Table S4]). Together, these data suggest that SARS-CoV-2 infection results in a coordinated change in the interferon signaling, inflammation, and mitochondrial processes.

Gene expression changes associated with SARS-CoV-2 infection is distinct from Influenza A virus infection with minor overlaps

SARS-CoV-2 vs Influenza A virus (IAV)

To compare the expression profile of SARS-CoV-2 infected cells with another virus infected cells, DE analysis of mock vs. influenza A virus (IAV) infected cells was performed and the up and downregulated genes are presented in a volcano plot (Supp Fig S4A, <https://doi.org/10.6084/m9.figshare.12272351> [Table S3]). The pathway analysis of the DE genes from this comparison showed enrichment in protein translation, localization and anti-viral responses (Supp Fig S4B, <https://doi.org/10.6084/m9.figshare.12272351> [Table S4]). Additionally, genes upregulated in the IAV infected cells annotated to pathways for virus response, protein trafficking, and unfolded protein response (UPR) (Fig 4A, <https://doi.org/10.6084/m9.figshare.12272351> [Table S4]). Genes that were downregulated in IAV infected cells enriched in vacuole and lysosome related processes (Fig 4B, <https://doi.org/10.6084/m9.figshare.12272351> [Table S4]). Interestingly, few DE genes from the

mock vs. SARS-CoV-2 overlapped with the DE genes from mock vs. IAV comparison (Supp Fig 4C).

A pathway enrichment summary map was created by overlaying the pathway enrichment results of the mock vs. IAV comparison on top of the mock vs. SARS-CoV-2 comparison. Consistent with the DE genes comparison (Supp Fig 4C), the enrichment map also highlighted little overlap of pathways between the two comparisons. DE genes from both comparisons commonly enriched in a subset of pathways associated with protein trafficking (Fig 4C). Furthermore, only a subset of the interferon pathway genes and a few chemokine genes that were upregulated in SARS-CoV-2 infected cells were also upregulated in IAV infected cells, while the autophagy and inflammation genes remained mostly unchanged in the latter (Fig 4D-F). Therefore, upregulation of cytokine/inflammation, changes in autophagy, and downregulation of the mitochondrial processes were uniquely observed in SARS-CoV-2 infected cells. Upregulation of DE genes involved in the cytokine/inflammation processes is consistent with cytokine storm observed in severe cases COVID-19 patients. Since these observations were made by analyzing the gene expression changes in a lung cell line, future studies profiling gene expression changes in severe COVID-19 patients will be needed to confirm these findings.

SARS-CoV-2 infected cells share some gene expression signature with MERS-CoV infected cells with few exceptions

SARS-CoV-2 vs MERS-CoV

Comparison of gene expression profiles revealed that a SARS-CoV-2 infected cells are distinct from those of IAV infected cells (Fig 4). Although these are both viruses, they are not phylogenetically close. Therefore, we next compared the gene expression profiles of SARS-CoV-2 and MERS-CoV infected cells, since both are hCoVs. DE analysis of the mock vs. SARS-CoV-2 infected Calu3 lung carcinoma cells identified several up and down genes (Supp Fig S5A, <https://doi.org/10.6084/m9.figshare.12272351> [Table S3]). Pathway enrichment analysis showed annotation of the DE genes to cell cycle, inflammation, apoptosis processes (Supp Fig S5B, <https://doi.org/10.6084/m9.figshare.12272351> [Table S4]). A pathway enrichment summary map for mock vs. SARS-CoV-2 and mock vs. MERS-CoV comparisons was generated to assess the extent of overlap of pathways between the two (Fig 5A). Notably, the DE genes from both comparisons enriched in the mitochondria, autophagy, cell cycle, and UPR

processes. However, DE genes from mock vs. SARS-CoV-2 comparison predominantly enriched in inflammation, cytokine signaling, and immunity related processes (Fig 5A). Consistently, genes upregulated in the SARS-CoV-2 infected Calu3 cells enriched in inflammation, nuclear factor kappaB (NFkB) processes (Fig 5B, <https://doi.org/10.6084/m9.figshare.12272351> [Table S4]), while upregulated genes from both hCoV infected cells annotated to protein trafficking and small GTPase signaling (Fig 5B, 5C, , <https://doi.org/10.6084/m9.figshare.12272351> [Table S4]). On the other hand, genes downregulated in both comparisons commonly annotated to mitochondrial processes (Fig 5D, 5E, <https://doi.org/10.6084/m9.figshare.12272351> [Table S4]). These findings suggest that perturbation of autophagy, mitochondrial genes are common gene expression signatures associated with hCoVs infection, but the SARS-CoV-2 virus almost exclusively impacts the cytokine/inflammatory processes in the lung cells. It is likely that perturbation of mitochondrial processes and autophagy may lead to a dysfunctional immune response (29, 30). Further studies will be required to understand if and how these processes may contribute to inflammation during SARS-CoV-2 infection.

Gene expression analysis of a severe Covid-19 lung sample shows exaggerated immune/inflammation response

Healthy vs. COVID-19 lung biopsy samples

The gene expression analysis of the SAR-CoV-2 infected cell lines suggested that the upregulation of the cytokine/inflammatory processes were uniquely impacted by this viral infection. To test if these processes were also impacted in COVID-19 lungs, RNA seq data from the healthy and COVID-19 lung biopsy were analyzed. The gene expression profile of a SARS-CoV-2 infected lung was distinct from healthy lungs with up and downregulated genes highlighted in the volcano plot (Supp Fig S6A, <https://doi.org/10.6084/m9.figshare.12272351> [Table S3]). The pathway enrichment summary map and the plot showed that the DE genes predominantly annotated to the inflammation, ROS, leukocyte/monocyte related pathways (Fig 6A, Supp Fig S6B). Furthermore, the DE genes upregulated in the COVID-19 lungs enriched in the anti-viral response processes, cytokine secretion, immune cell proliferation/migration, and inflammation (Fig 6B, <https://doi.org/10.6084/m9.figshare.12272351> [Table S4]). The downregulated genes were significantly enriched in protein trafficking, RNA metabolism, and oxygen sensing processes (Fig 6C, <https://doi.org/10.6084/m9.figshare.12272351> [Table S4]). It

is likely that the perturbations in the oxygen sensing processes are reflective of the severe respiratory distress often seen in severe COVID-19 patients to due reduced oxygenation ability of the failing lungs.

To further assess the role of immune/lung cell types in COVID-19, lung sc RNA seq data was analyzed to identify marker genes enriched in different cell types (Supp Fig S6C). Several marker genes were identified from the alveolar epithelial type I/II, T-lymphocytes, monocytes and macrophages subpopulation. Of these, marker genes from the monocytes and macrophage cell types were differentially expressed in COVID-19 lungs compared with healthy lungs (Fig. 6D, Supp Table 2). Together, these results support a critical role for inflammatory signaling likely arising partly from the monocyte/macrophage immune cell population in COVID-19 pathogenesis. These data are consistent with the findings from SARS-CoV-2 infected lung cell lines.

DISCUSSION

Highly pathogenic human coronaviruses (hCoV) are known to infect the lower respiratory airways and cause severe acute respiratory syndrome (SARS) (14). The recently discovered SARS-CoV-2 virus is the cause of COVID-19 (31). The clinical manifestations of this virus infection include fever, cough, fatigue, respiratory distress, and cardiac injury (32-34). While some patients with COVID-19 suffered from mild symptoms, other patients had increasingly life-threatening symptoms (34). Age and underlying medical conditions such as diabetes, hypertension, are likely to determine the severity of the symptoms (35). However, the underlying biological processes and mechanisms impacted by this viral infection of the host is still not clear. Analyzing the gene expression profiles of host cells infected with SARS-CoV-2 will be necessary to decipher the subcellular functions perturbed by this virus and to inform drug development strategies.

Here we present an in-depth differential expression analysis of A549 and Calu3 cell lines, comparing mock to infection with either SARS-CoV-2, or IAV, or MERS-CoV. We conclude that (i) SARS-CoV-2 infection of the cells at higher titer likely represents a severe COVID-19 infection state; (ii) the gene expression profile of SARS-CoV-2 infected cells were distinct from that of the IAV infected cells. Specifically, SARS-CoV-2 infection impacted the expression of

genes in inflammation, cell cycle, reactive oxygen species (ROS), autophagy, and mitochondrial processes, which were absent in IAV infected cells; (iii) comparing the expression profile of SARS-CoV-2 and MERS-CoV infected cells revealed that perturbation in autophagy and mitochondrial processes is common in hCoV infections. However, increased expression of the inflammatory/cytokine signaling genes were exclusively observed in SARS-CoV-2 infected lung cells. Together, these data suggest that perturbation in the autophagy, mitochondrial processes in SARS-CoV-2 infected lung cells could hinder an effective immune response (29, 30) and increase inflammation, which is often seen in severe COVID-19 patients suffering from cytokine storm (14, 36). Since these conclusions were made using the data from virus infected lung cell lines, the correlation between these cells' expression profiles and marker genes expression from different lung cell types were determined. While the A549 cells showed robust correlation with lung epithelial lineage basal and ionocyte cells, Calu3 cells showed similar pattern but lower correlation with these cell types. Therefore, the processes delineated in SARS-CoV-2 A549 cells likely represent the lung epithelial cells response to SARS-CoV-2 infection. To further substantiate these findings, however, gene expression profiling of lung samples from patients with mild or severe COVID-19 will be required to confirm these findings. Nevertheless, this analysis has delineated several biological processes, discussed in more detail below, that are impacted in the SARS-CoV-2 infected host cells.

SARS-CoV-2 infection at both low and high titer upregulated the expression of genes in cytokines and interferon signaling in the host cells. Additionally, SARS-CoV-2 infection at low viral titer also upregulated complement genes and receptor mediated endocytosis. While the former is critical for defense against viral infection, and activation of inflammatory processes (37, 38); latter is required for viral entry (39, 40). Notably, some complement genes (C1S, C1R) are upregulated in high viral titer SARS-CoV-2 infected cells. Consistently, the C1q/TNF-related protein 6, a glycoprotein that regulates complement activation, is downregulated in SARS-CoV-2 infected cells. This gene is implicated in arthritis, and intra-articular injection of the recombinant C1qTNF6 protein was shown as an effective strategy in improving arthritis and inflammation in C1qtnf6^{-/-} mice (41). An elevated complement response could likely lead to excessive inflammation, which was also observed in MERS-CoV infection of the hDPP4-transgenic mouse model (42). These observations suggest that inhibition of the complement

system or the receptor mediated endocytosis processes as potential treatment strategies could be tested.

Infection of SARS-CoV-2 at higher viral titer perturbed autophagy, upregulated genes in the interferon, cytokine, nuclear factor kappaB (NFkB), reactive oxygen species (ROS) processes, while downregulated the genes in the mitochondrial, electron transport chain processes. Consistently, analysis of DE genes in one of the correlated clusters from WGCNA showed significant enrichment in the interferon signaling processes. Additionally, GeneMANIA analysis of the correlated DE genes in two modules revealed PPI subnetworks of genes involved in interferon stimulated genes (ISGs) and NFkB, which were both mostly upregulated in the infected cells. In addition to the ISGs, the JAK-STAT signal transduction genes, which play critical role in type I cytokine (such as IL6) signaling and inflammation (43-45), were also upregulated in the SARS-CoV-2 infected cells (Fig 4C). IL6, a pleotropic cytokine, was shown to be elevated in critically ill COVID-19 patients (46). Consistently, IL6 was upregulated in the SARS-CoV-2 infected cells. IL6 acts via the JAK-STAT signaling through SOCS3 protein kinase (also upregulated in SARS-CoV-2 infected cells) to activate the immune response (47). Excessive IL6 causes excessive inflammation as seen in arthritis (48). Additionally, three IL1 family cytokines IL1a, IL1b and IL36b were also upregulated in SARS-CoV-2 infected cells. IL1 signaling is critical for initiating and regulating inflammatory processes in response to infection (49, 50). Given the upregulation of genes in the cytokine/inflammatory processes was predominantly seen in cells infected with SARS-CoV-2 at higher viral titer, it is likely that these cells represent a severe COVID-19 infection state. Upregulation of IL6, IL1, and NFkB genes may be contribute to the inflammatory symptoms observed in severe COVID-19 patients (14, 36). Consistent with the data from lung cell lines, genes upregulated in COVID-19 lung biopsy samples were also significantly enriched in cytokine/inflammatory processes. These data support a central role for cytokine signaling in COVID-19 pathogenesis. Therefore, treatment strategies aimed at mitigating the cytokine effects or complement system could be tested in treatment of COVID-19. One such clinical trial aimed at mitigating the IL6 effects is already underway (NCT04322773).

What processes may be causing/contributing to the activation of the inflammatory processes in the SARS-CoV-2 infected cells? Mitochondria and autophagy related processes

were two other prominent categories of the biological processes that were exclusively impacted in the hCoV infected cells.

Viruses are known to either induce or inhibit various mitochondrial processes as part of their replication and dissemination efforts (51). Infection of cells with SARS-CoV-2 at higher viral titer downregulated the genes in the mitochondrial processes. Consistently, WGCNA also identified a DE gene cluster that annotated to the mitochondrial organization and translation processes. Subsequent GeneMANIA analysis identified a PPI subnetwork of genes involved in mitochondrial translation which were coordinately downregulated in SARS-CoV-2 infected cells. Since mitochondrial import and translation are inter-linked (52, 53), we found that several mitochondrial complex I and translocase genes were downregulated in the SARS-CoV-2 infected cells. Reduced complex I expression has been found in many cancer cells and is shown to affect the oxidative phosphorylation, which also impacts the immune cell function (30, 54-57). Together, these data highlight that several mitochondrial processes were impacted, which in turn could perturb the immune response processes in SARS-Cov-2 infected cells.

In parallel with the mitochondrial processes, autophagic processes were perturbed in cells infected with SARS-CoV-2 at high titer. The positive-sense RNA viruses (such as hCoVs) may utilize the autophagy pathway to fabricate membrane structures required for viral replication (58). This ambivalence between anti-viral and pro-viral roles (59) may explain why SARS-CoV-2 infected cells exhibited both up- and downregulation of autophagy pathway genes. However, the precise role of autophagy in coronavirus infection remains unclear (58). The gene expression analysis of SARS-CoV-2 infected cells showed upregulation of autophagy nucleation genes ATG5, ATG12, and LC3I. This is consistent with the previous reports showing autophagy induction in coronavirus infected cells (60). Moreover, coronavirus mouse hepatitis virus (MHV) replication was impaired in *atg5*^{-/-} cells (60). Finally, inhibition of S-phase kinase-associated protein 2 (SKP2) as E3 ligase decreased Beclin1 (BECN1) degradation, and increased autophagic flux, which in turn decreased MERS-CoV (39, 61). However, SKP2 expression in SARS-CoV-2 infected cells is significantly low. Further studies will be required to fully understand the interplay between autophagy and SARS-CoV-2 infection.

SUMMARY

In summary, we have presented a detailed DE and coexpression network analysis of the RNA seq data from SARS-CoV-2 infected cells. This analysis has delineated biological processes impacted during SARS-CoV-2 infection of lung cells. Notably, we saw upregulation of genes in the cytokine signaling and inflammation processes, downregulation of genes in the mitochondrial processes, and perturbation of autophagy. It is likely that perturbation of autophagy and mitochondrial processes may impede an effective immune response leading to severe outcomes. Consistent with the SARS-CoV-2 infected cells gene expression profile, RNA seq analysis of COVID-19 lung biopsy sample also supports a central role for cytokine/inflammation processes in COVID-19 pathogenesis. These findings provide some insights into mechanisms potentially contributing to dysregulated immune responses that are observed in severe COVID-19 patients. Since these studies used the gene expression data from lung cell lines, future studies analyzing the gene expression profile of COVID-19 patient samples will be required to confirm these findings.

MATERIALS AND METHODS

Data collection

Raw gene count matrix for bulk RNA-seq was downloaded from GEO (accession number GSE147507) (62). The data contained gene expression count matrix of two lung carcinoma cell lines A549 (63, 64) and Calu3 (65, 66). In this dataset, the A549 treatment conditions included mock, infection with influenza A virus (IAV) (N=2 per group), and infection with SARS-CoV-2 at 2 (high titer, N=3 per group) and 0.2 (low titer, N=3 per group) multiplicity of infection (MOI). From this dataset the raw gene count matrix for 2 healthy human lung biopsy and one COVID-19 samples (2 technical replicates) were also analyzed. Additionally, gene expression data in FPKM was downloaded from GEO (accession number GSE139516) (67) for Calu3 cell line infected with MERS-CoV and mock (N=3 per group). Differential expression (DE) analysis was performed on mock and MERS-CoV infected cells for 24 hr. Human lung single-cell RNA-seq (scRNA-seq) data with 57 annotated cell types was downloaded from Synapse (accession syn21041850) (68).

Data analysis

RNA seq analysis and network analysis

Differential expression analysis was performed using limma-voom and limma trends (69, 70). Genes with adjusted p value < 0.05 were considered differentially expressed (DE). The DE genes were tested for pathway enrichment using clusterProfiler and pathways with q value < 0.05 were considered significant (71). Consensus weighted gene coexpression network analysis (WGCNA) (27) was performed on pooled control and SARS-CoV-2 infected cells at low and high titer expression data, after removing the low expressing genes with count less than 5 in 4/6 samples. DE genes in correlated modules > 50 genes in size were selected for downstream analysis. For subnetwork analysis, GeneMANIA database (72) was used to identify potential protein-protein interaction (PPI) between the DE genes from the correlated modules. The PPI networks were then overlaid with the fold-change information using Cytoscape (73). Pathway enrichment summary amp was generated using the Enrichment Map (74) and AutoAnnotate (75) apps in Cytoscape. R (Foundation for Statistical Computing, Vienna, Austria. URL <https://www.R-project.org/>) was used for data visualization.

The data sets supporting the results of this article are available from Figshare (<https://doi.org/10.6084/m9.figshare.12272351>) (76).

Single-cell RNA-seq analysis

Analysis of human lung single-cell RNA-seq (scRNA-seq) data with 57 annotated cell types was performed in R (v3.6) using Seurat (v3.1.1) (77). The UMI (Unique Molecular Identifier) count matrix was filtered for genes expressed in less than 3 cells and normalized using *SCTransform* implemented in Seurat. Differentially expressed genes were computed for 57 cell types using *FindAllMarkers* implemented in Seurat with default parameters. The UMAP plot was plotted using the top 50 principal components computed from the expression of highly variable genes selected by *SCTransform*.

Correlation of expression profiles between cell lines and lung cell types

To assess the biological significance of analyzing expression profiles of lung cell lines, we compared the expression profile of A549 and Calu3 cell lines with that of lung cell types. Using the scRNA seq data, cell type expression profile was computed as the mean expression

across cells within each cell type. The top 1000 genes with the highest variance among the 57 cell type expression profiles were selected as highly variable genes which were presumably informative for differentiating the 57 cell types. This analysis revealed that the A549 cells gene expression strongly correlated with the basal and ionocyte lung cell subpopulations, which both represent lung epithelial cell lineage (22, 23). Correlation between the highly variable genes from lung scRNA seq data and either A549 or Calu3 cells were calculated and plotted (Supp Fig S7A). Notably, the Calu3 cells showed similar pattern but lower correlation with the lung cell types analyzed (Supp Fig S7A).

Acknowledgements

We thank Dr. Mark Knepper, head of the Epithelial Systems Biology Laboratory at the NHLBI, for providing his input in data analysis. This work utilized the computational resources of the NIH HPC Biowulf cluster (<http://hpc.nih.gov>). This work was supported by the Intramural Research Programs (IRPs) of the National Heart, Lung, and Blood Institute (NHLBI).

Figure legends

Figure 1: SARS-CoV-2 infection of lung epithelial cells impacts expression of genes in interferon, cytokine and autophagic processes. (A) Pathway enrichment analysis of gene upregulated in SARS-CoV-2 infected cell. (B) Heatmap highlighting the expression of genes in the cytokine processes in mock and infected cells. (C) Heatmap highlighting the expression of genes in the autophagic processes in mock and infected cells. (D) Heatmap highlighting the expression of genes in the interferon related processes in mock and infected cells. (E) Pathway enrichment analysis of gene upregulated in SARS-CoV-2 infection. (F) Heatmap highlighting the expression of genes in the mitochondrial organization and translation in mock and infected cells. (G) Pathway enrichment summary map for mock vs. SARS-CoV-2 at high MOI (blue nodes) and low MOI (red nodes) comparisons. Single color nodes are pathways that are distinctly enriched by DE genes from one comparison (single color node). Two colored nodes are pathways enriched by DE genes from both comparisons. Each node represents a pathway/biological process (BP). The node size is proportional to the number of DE genes overlapping with the BP. The nodes that share genes are connected with edges. The black circle summarizes the gene ontology (GO) terms of similar BPs. Mock vs. SARS-CoV-2 (high MOI) DE genes exclusively enriched in inflammation, interferon, autophagy and mitochondria related processes. Mock vs. SARS-CoV-2 (low MOI) DE genes exclusively enriched in ECM/blood, receptor mediated endocytosis, and nucleotide biosynthesis processes. MOI: multiplicity of infection; DE: differentially expressed.

Figure 2: ACE2 overexpression (oe) exacerbates the expression fold change of genes in the inflammation and mitochondria/respiration processes. (A) Overlap of DE genes after SARS-CoV-2 infection with or without ACE2 overexpression. Fraction of upregulated or downregulated genes that were further exacerbated by ACE2 oe is indicated. (B) Pathway enrichment analysis of DE genes further upregulated after SARS-CoV-2 infection in ACE2 oe cells. (C) Pathway enrichment analysis of DE genes further downregulated regulated after SARS-CoV-2 infection in ACE2 oe cells. DE: differentially expressed.

Figure 3: Consensus network analysis of mock and SARS-CoV-2 infected (high and low MOI) cells. (A) Cluster dendrogram showing correlated genes grouped into clusters marked by different colors on the horizontal block labeled “Consensus Module Colors”. The DE genes in each cluster is marked as black color vertical line in the horizontal block labeled “DE genes”. The up and down regulated genes are shown as red and blue color vertical lines in a block labeled “Upregulated/downregulated genes”, respectively. (B) Pathway enrichment analysis of correlated DE genes in the turquoise module. (C) Protein-protein interaction (PPI) subnetworks in the turquoise module is presented where each node represents a gene and the border color of the nodes indicate up (red color) and downregulation (blue) in infected cells compared to mock infected cells. The edge between the nodes indicate interaction based on the GeneMANIA database information. The network shows interferon stimulated genes and inflammatory genes. (D) Another PPI subnetwork identified in the turquoise module showing several mitochondrial genes. (E) Pathway enrichment analysis of correlated DE genes in the blue module. (F) A PPI subnetwork of correlated DE genes in the blue module showing a well-connected interactome of genes involved in inflammation. DE: differentially expressed.

Figure 4: SARS-CoV-2 infection of A549 lung epithelial cells results in distinct gene expression changes that are not seen in IAV infection. (A) Pathway enrichment analysis of DE genes upregulated in IAV infected cells. (B) Pathway enrichment analysis of DE genes downregulated in IAV infected cells. (C) Pathway enrichment summary map for mock vs. SARS-CoV-2 (blue nodes) and mock vs. IAV (red nodes) comparisons. Single color nodes are pathways that are distinctly enriched by DE genes from one comparison. Two colored nodes are pathways enriched by DE genes from both comparisons. Each node represents a pathway/biological process (BP). The node size is proportional to the number of DE genes overlapping with the BP. The nodes that share genes are connected with edges. The black circle summarizes the gene ontology (GO) terms of similar BPs. DE genes from Mock vs. SARS-CoV-2 comparison exclusively enriched in inflammation, interferon, autophagy and mitochondria related processes. (D) Volcano plot of mock vs. IAV infected cells showing cytokine related genes. (E) Volcano plot of mock vs. IAV infected cells showing autophagy related genes. (F) Volcano plot of mock vs. IAV infected cells showing interferon related genes. DE: differentially expressed.

Figure 5: SARS-CoV-2 and MERS-CoV infection have some common and some distinct gene expression signatures. (A) Pathway enrichment summary map for mock vs. SARS-CoV-2 (blue nodes) and mock vs. MERS-CoV (red nodes) comparisons. Single color nodes are pathways that are distinctly enriched by DE genes from one comparison (single color node). Two colored nodes are pathways enriched by DE genes from both comparisons. Each node represents a pathway/biological process (BP). The node size is proportional to the number of DE genes

overlapping with the BP. The nodes that share genes are connected with edges. The black circle outlines group the gene ontology (GO) terms of similar BPs. The DE genes from mock vs. SARS-CoV-2 predominantly enriched in inflammation and immunity related processes. (B) Pathway enrichment analysis of DE genes upregulated in SARS-CoV-2 infected Calu3 cells. (C) Pathway enrichment analysis of DE genes upregulated in MERS-CoV infected Calu3 cells. (D) Pathway enrichment analysis of DE genes downregulated in SARS-CoV-2 infected Calu3 cells. (E) Pathway enrichment analysis of DE genes downregulated in MERS-CoV infected Calu3 cells. DE: differentially expressed.

Figure 6: DE genes from Covid-19 lung compared to healthy lungs show robust upregulation of immunity, cytokines, and inflammatory processes. (A) Pathway enrichment summary map for healthy vs. Covid-19 lungs (technical replicates) (blue nodes). Each node represents a pathway/biological process (BP). The node size is proportional to the number of DE genes overlapping with the BP. The nodes that share genes are connected with edges. The black circle summarizes the gene ontology (GO) terms of similar BPs. The DE genes from healthy vs. Covid-19 lung comparison predominantly enriched in inflammation and immunity related processes. (B) Pathway enrichment analysis of DE genes upregulated in Covid-19 lung vs. healthy lung biopsy samples. (C) Pathway enrichment analysis of DE genes downregulated in Covid-19 lung vs. healthy lung biopsy samples (D) UMAP visualization colored by cell types. DE: differentially expressed.

Supplemental Figure Legend

Supp Fig S1. (A) Volcano plot showing up (red color dots) and down regulated (blue color dots) DE genes in mock vs. SARS-CoV-2 (high MOI) infected A549 cells. (B) Pathway enrichment analysis of the DE genes from the mock vs. SARS-CoV-2 (high MOI) comparison. (C) Volcano plot showing up (red color dots) and down regulated (blue color dots) DE genes in mock vs. SARS-CoV-2 (low MOI) infected A549 cells. (D) Pathway enrichment analysis of the DE genes from the mock vs. SARS-CoV-2 (low MOI) comparison. DE: differentially expressed; MOI: multiplicity of infection.

Supp Fig S2. (A) Volcano plot showing up (red color dots) and down regulated (blue color dots) genes in A549 cells overexpressing ACE2 infected with. SARS-CoV-2 (low MOI) or mock treatment. (B) Pathway enrichment analysis of DE genes from mock vs. SARS-CoV-2 in ACE2 oe cells. (C) Venn diagram showing overlap between DE genes from mock vs. SARS-CoV-2 (low MOI) and mock vs. SARS-CoV-2 (in ACE2 oe) comparisons. oe: overexpressing; DE: differentially expressed; MOI: multiplicity of infection.

Supp Fig S3. (A) Pathway enrichment analysis of correlated DE genes in the brown consensus module. DE: differentially expressed.

Supp Fig S4. (A) Volcano plot showing up (red color dots) and down regulated (blue color dots) DE genes in mock vs. IAV infected A549 cells. (B) Pathway enrichment analysis of the DE genes from the mock vs. IAV comparison. (C) Venn diagram showing DE genes overlap between mock vs. SARS-CoV-2 (High MOI) and mock vs. IAV comparisons. DE: differentially expressed; MOI: multiplicity of infection.

Supp Fig S5. (A) Volcano plot showing up (red color dots) and down regulated (blue color dots) DE genes in mock vs. SAR-CoV-2 infected Calu3 cells. (B) Pathway enrichment analysis of the DE genes from the mock vs. SAR-CoV-2 comparison. DE: differentially expressed.

Supp Fig S6. (A) Volcano plot showing up (red color dots) and down regulated (blue color dots) DE genes in healthy vs. COVID-19 lung biopsy samples comparison. (B) Pathway enrichment analysis of the DE genes from the healthy vs. COVID-19 lung biopsy samples comparison. (C) tSNE plot of lung single cell (sc) RNA seq data. DE: differentially expressed.

Supp Fig S7. (A) Plot showing correlation between marker genes from different lung subpopulations (on x-axis) and A549 and Calu3 cells lines (color coded independent samples with legend on the right side of the plot).

[Supplemental Tables](#)

Supp Table 1: Consensus module name and size (gene numbers) and its overlap with significant genes

Supp Table 2: List of marker genes of lung cell types from single cell RNA-seq data

REFERENCES

1. Cascella M, Rajnik M, Cuomo A, Dulebohn SC, Di Napoli R. 2020. Features, Evaluation and Treatment Coronavirus (COVID-19), StatPearls, Treasure Island (FL).
2. Fung SY, Yuen KS, Ye ZW, Chan CP, Jin DY. 2020. A tug-of-war between severe acute respiratory syndrome coronavirus 2 and host antiviral defence: lessons from other pathogenic viruses. *Emerg Microbes Infect* 9:558-570.
3. Yuen KS, Ye ZW, Fung SY, Chan CP, Jin DY. 2020. SARS-CoV-2 and COVID-19: The most important research questions. *Cell Biosci* 10:40.
4. World Health Organization. 2020. Coronavirus disease (COVID-19) Pandemic. <https://www.who.int/emergencies/diseases/novel-coronavirus-2019>. Accessed April 27, 2020.
5. Raoult D, Zumla A, Locatelli F, Ippolito G, Kroemer G. 2020. Coronavirus infections: Epidemiological, clinical and immunological features and hypotheses. *Cell Stress* 4:66-75.
6. de Wit E, van Doremalen N, Falzarano D, Munster VJ. 2016. SARS and MERS: recent insights into emerging coronaviruses. *Nat Rev Microbiol* 14:523-34.
7. Wu A, Peng Y, Huang B, Ding X, Wang X, Niu P, Meng J, Zhu Z, Zhang Z, Wang J, Sheng J, Quan L, Xia Z, Tan W, Cheng G, Jiang T. 2020. Genome Composition and Divergence of the Novel Coronavirus (2019-nCoV) Originating in China. *Cell Host Microbe* 27:325-328.
8. Zhang YZ, Holmes EC. 2020. A Genomic Perspective on the Origin and Emergence of SARS-CoV-2. *Cell* 181:223-227.
9. Katze MG, Fornek JL, Palermo RE, Walters KA, Korth MJ. 2008. Innate immune modulation by RNA viruses: emerging insights from functional genomics. *Nat Rev Immunol* 8:644-54.
10. Blanco-Melo D, Nilsson-Payant BE, Liu W-C, Møller R, Panis M, Sachs D, Albrecht RA, tenOever BR. 2020. SARS-CoV-2 launches a unique transcriptional signature from in vitro, ex vivo, and in vivo systems. *bioRxiv*.
11. Grove J, Marsh M. 2011. The cell biology of receptor-mediated virus entry. *J Cell Biol* 195:1071-82.
12. Mar KB, Rinkenberger NR, Boys IN, Eitson JL, McDougal MB, Richardson RB, Schoggins JW. 2018. LY6E mediates an evolutionarily conserved enhancement of virus infection by targeting a late entry step. *Nat Commun* 9:3603.
13. Chen G, Wu D, Guo W, Cao Y, Huang D, Wang H, Wang T, Zhang X, Chen H, Yu H, Zhang X, Zhang M, Wu S, Song J, Chen T, Han M, Li S, Luo X, Zhao J, Ning Q. 2020. Clinical and immunological features of severe and moderate coronavirus disease 2019. *J Clin Invest* doi:10.1172/JCI137244.
14. Channappanavar R, Perlman S. 2017. Pathogenic human coronavirus infections: causes and consequences of cytokine storm and immunopathology. *Semin Immunopathol* 39:529-539.
15. Liao M, Liu Y, Yuan J, Wen Y, Xu G, Zhao J, Chen L, Li J, Wang X, Wang F, Liu L, Zhang S, Zhang Z. 2020. The landscape of lung bronchoalveolar immune cells in COVID-19 revealed by single-cell RNA sequencing. *medRxiv*.

16. Rockx B, Kuiken T, Herfst S, Bestebroer T, Lamers MM, de Meulder D, van Amerongen G, van den Brand J, Okba NMA, Schipper D, van Run P, Leijten L, Verschoor E, Verstrepen B, Langermans J, Drosten C, van Vliissingen MF, Fouchier R, de Swart R, Koopmans M, Haagmans BL. 2020. Comparative Pathogenesis Of COVID-19, MERS And SARS In A Non-Human Primate Model. *bioRxiv*.
17. To KF, Tong JH, Chan PK, Au FW, Chim SS, Chan KC, Cheung JL, Liu EY, Tse GM, Lo AW, Lo YM, Ng HK. 2004. Tissue and cellular tropism of the coronavirus associated with severe acute respiratory syndrome: an in-situ hybridization study of fatal cases. *J Pathol* 202:157-63.
18. Chu H, Chan JF-W, Yuen TT-T, Shuai H, Yuan S, Wang Y, Hu B, Yip CC-Y, Tsang JO-L, Huang X, Chai Y, Yang D, Hou Y, Chik KK-H, Zhang X, Fung AY-F, Tsoi H-W, Cai J-P, Chan W-M, Ip JD, Chu AW-H, Zhou J, Lung DC, Kok K-H, To KK-W, Tsang OT-Y, Chan K-H, Yuen K-Y. 2020. Comparative tropism, replication kinetics, and cell damage profiling of SARS-CoV-2 and SARS-CoV with implications for clinical manifestations, transmissibility, and laboratory studies of COVID-19: an observational study. *The Lancet Microbe* doi:[https://doi.org/10.1016/S2666-5247\(20\)30004-5](https://doi.org/10.1016/S2666-5247(20)30004-5).
19. Ziegler CGK, Allon SJ, Nyquist SK, Mbanjo IM, Miao VN, Tzouanas CN, Cao Y, Yousif AS, Bals J, Hauser BM, Feldman J, Muus C, Wadsworth MH, Kazer SW, Hughes TK, Doran B, Gatter GJ, Vukovic M, Taliaferro F, Mead BE, Guo Z, Wang JP, Gras D, Plaisant M, Ansari M, Angelidis I, Adler H, Sucre JMS, Taylor CJ, Lin B, Waghray A, Mitsialis V, Dwyer DF, Buchheit KM, Boyce JA, Barrett NA, Laidlaw TM, Carroll SL, Colonna L, Tkachev V, Peterson CW, Yu A, Zheng HB, Gideon HP, Winchell CG, Lin PL, Bingle CD, Snapper SB, Kropski JA, Theis FJ, et al. 2020. SARS-CoV-2 receptor ACE2 is an interferon-stimulated gene in human airway epithelial cells and is detected in specific cell subsets across tissues. *Cell* doi:<https://doi.org/10.1016/j.cell.2020.04.035>.
20. Zhou L, Niu Z, Jiang X, Zhang Z, Zheng Y, Wang Z, Zhu Y, Gao L, Wang X, Sun Q. 2020. Systemic analysis of tissue cells potentially vulnerable to SARS-CoV-2 infection by the protein-proofed single-cell RNA profiling of ACE2, TMPRSS2 and Furin proteases. *bioRxiv* doi:10.1101/2020.04.06.028522:2020.04.06.028522.
21. Hoffmann M, Kleine-Weber H, Schroeder S, Kruger N, Herrler T, Erichsen S, Schiergens TS, Herrler G, Wu NH, Nitsche A, Muller MA, Drosten C, Pohlmann S. 2020. SARS-CoV-2 Cell Entry Depends on ACE2 and TMPRSS2 and Is Blocked by a Clinically Proven Protease Inhibitor. *Cell* 181:271-280 e8.
22. Morrisey EE. 2018. Basal Cells in Lung Development and Repair. *Dev Cell* 44:653-654.
23. Schiller HB, Montoro DT, Simon LM, Rawlins EL, Meyer KB, Strunz M, Vieira Braga FA, Timens W, Koppelman GH, Budinger GRS, Burgess JK, Waghray A, van den Berge M, Theis FJ, Regev A, Kaminski N, Rajagopal J, Teichmann SA, Misharin AV, Nawijn MC. 2019. The Human Lung Cell Atlas: A High-Resolution Reference Map of the Human Lung in Health and Disease. *Am J Respir Cell Mol Biol* 61:31-41.
24. Shang J, Ye G, Shi K, Wan Y, Luo C, Aihara H, Geng Q, Auerbach A, Li F. 2020. Structural basis of receptor recognition by SARS-CoV-2. *Nature* doi:10.1038/s41586-020-2179-y.
25. Xu X, Chen P, Wang J, Feng J, Zhou H, Li X, Zhong W, Hao P. 2020. Evolution of the novel coronavirus from the ongoing Wuhan outbreak and modeling of its spike protein for risk of human transmission. *Sci China Life Sci* 63:457-460.

26. Li W, Sui J, Huang IC, Kuhn JH, Radoshitzky SR, Marasco WA, Choe H, Farzan M. 2007. The S proteins of human coronavirus NL63 and severe acute respiratory syndrome coronavirus bind overlapping regions of ACE2. *Virology* 367:367-74.
27. Langfelder P, Horvath S. 2008. WGCNA: an R package for weighted correlation network analysis. *BMC Bioinformatics* 9:559.
28. Franz M, Rodriguez H, Lopes C, Zuberi K, Montojo J, Bader GD, Morris Q. 2018. GeneMANIA update 2018. *Nucleic Acids Res* 46:W60-W64.
29. Jang YJ, Kim JH, Byun S. 2019. Modulation of Autophagy for Controlling Immunity. *Cells* 8.
30. Won JH, Park S, Hong S, Son S, Yu JW. 2015. Rotenone-induced Impairment of Mitochondrial Electron Transport Chain Confers a Selective Priming Signal for NLRP3 Inflammasome Activation. *J Biol Chem* 290:27425-37.
31. Tamarro A, Adebajo GAR, Parisella FR, Pezzuto A, Rello J. 2020. Cutaneous manifestations in COVID-19: the experiences of Barcelona and Rome. *J Eur Acad Dermatol Venereol* doi:10.1111/jdv.16530.
32. Chen N, Zhou M, Dong X, Qu J, Gong F, Han Y, Qiu Y, Wang J, Liu Y, Wei Y, Xia J, Yu T, Zhang X, Zhang L. 2020. Epidemiological and clinical characteristics of 99 cases of 2019 novel coronavirus pneumonia in Wuhan, China: a descriptive study. *Lancet* 395:507-513.
33. Huang C, Wang Y, Li X, Ren L, Zhao J, Hu Y, Zhang L, Fan G, Xu J, Gu X, Cheng Z, Yu T, Xia J, Wei Y, Wu W, Xie X, Yin W, Li H, Liu M, Xiao Y, Gao H, Guo L, Xie J, Wang G, Jiang R, Gao Z, Jin Q, Wang J, Cao B. 2020. Clinical features of patients infected with 2019 novel coronavirus in Wuhan, China. *Lancet* 395:497-506.
34. Guan W-j, Ni Z-y, Hu Y, Liang W-h, Ou C-q, He J-x, Liu L, Shan H, Lei C-l, Hui DSC, Du B, Li L-j, Zeng G, Yuen K-Y, Chen R-c, Tang C-l, Wang T, Chen P-y, Xiang J, Li S-y, Wang J-l, Liang Z-j, Peng Y-x, Wei L, Liu Y, Hu Y-h, Peng P, Wang J-m, Liu J-y, Chen Z, Li G, Zheng Z-j, Qiu S-q, Luo J, Ye C-j, Zhu S-y, Zhong N-s. 2020. Clinical Characteristics of Coronavirus Disease 2019 in China. *New England Journal of Medicine* doi:10.1056/NEJMoa2002032.
35. Wang D, Hu B, Hu C, Zhu F, Liu X, Zhang J, Wang B, Xiang H, Cheng Z, Xiong Y, Zhao Y, Li Y, Wang X, Peng Z. 2020. Clinical Characteristics of 138 Hospitalized Patients With 2019 Novel Coronavirus-Infected Pneumonia in Wuhan, China. *JAMA* doi:10.1001/jama.2020.1585.
36. Mehta P, McAuley DF, Brown M, Sanchez E, Tattersall RS, Manson JJ, Hlh Across Speciality Collaboration UK. 2020. COVID-19: consider cytokine storm syndromes and immunosuppression. *Lancet* 395:1033-1034.
37. Agrawal P, Nawadkar R, Ojha H, Kumar J, Sahu A. 2017. Complement Evasion Strategies of Viruses: An Overview. *Front Microbiol* 8:1117.
38. Dunkelberger JR, Song WC. 2010. Complement and its role in innate and adaptive immune responses. *Cell Res* 20:34-50.
39. Yang N, Shen HM. 2020. Targeting the Endocytic Pathway and Autophagy Process as a Novel Therapeutic Strategy in COVID-19. *Int J Biol Sci* 16:1724-1731.
40. Wang H, Yang P, Liu K, Guo F, Zhang Y, Zhang G, Jiang C. 2008. SARS coronavirus entry into host cells through a novel clathrin- and caveolae-independent endocytic pathway. *Cell Res* 18:290-301.

41. Murayama MA, Kakuta S, Inoue A, Umeda N, Yonezawa T, Maruhashi T, Tateishi K, Ishigame H, Yabe R, Ikeda S, Seno A, Chi HH, Hashiguchi Y, Kurata R, Tada T, Kubo S, Sato N, Liu Y, Hattori M, Saijo S, Matsushita M, Fujita T, Sumida T, Iwakura Y. 2015. CTRP6 is an endogenous complement regulator that can effectively treat induced arthritis. *Nat Commun* 6:8483.
42. Jiang Y, Zhao G, Song N, Li P, Chen Y, Guo Y, Li J, Du L, Jiang S, Guo R, Sun S, Zhou Y. 2018. Blockade of the C5a-C5aR axis alleviates lung damage in hDPP4-transgenic mice infected with MERS-CoV. *Emerg Microbes Infect* 7:77.
43. O'Brown ZK, Van Nostrand EL, Higgins JP, Kim SK. 2015. The Inflammatory Transcription Factors NFkappaB, STAT1 and STAT3 Drive Age-Associated Transcriptional Changes in the Human Kidney. *PLoS Genet* 11:e1005734.
44. Leonard WJ, O'Shea JJ. 1998. Jaks and STATs: biological implications. *Annu Rev Immunol* 16:293-322.
45. Banerjee S, Biehl A, Gadina M, Hasni S, Schwartz DM. 2017. JAK-STAT Signaling as a Target for Inflammatory and Autoimmune Diseases: Current and Future Prospects. *Drugs* 77:521-546.
46. Chen X, Zhao B, Qu Y, Chen Y, Xiong J, Feng Y, Men D, Huang Q, Liu Y, Yang B, Ding J, Li F. 2020. Detectable serum SARS-CoV-2 viral load (RNAemia) is closely associated with drastically elevated interleukin 6 (IL-6) level in critically ill COVID-19 patients. medRxiv.
47. Brocke-Heidrich K, Kretzschmar AK, Pfeifer G, Henze C, Loffler D, Koczan D, Thiesen HJ, Burger R, Gramatzki M, Horn F. 2004. Interleukin-6-dependent gene expression profiles in multiple myeloma INA-6 cells reveal a Bcl-2 family-independent survival pathway closely associated with Stat3 activation. *Blood* 103:242-51.
48. Srirangan S, Choy EH. 2010. The role of interleukin 6 in the pathophysiology of rheumatoid arthritis. *Ther Adv Musculoskelet Dis* 2:247-56.
49. Singer JW, Fleischman A, Al-Fayoumi S, Mascarenhas JO, Yu Q, Agarwal A. 2018. Inhibition of interleukin-1 receptor-associated kinase 1 (IRAK1) as a therapeutic strategy. *Oncotarget* 9:33416-33439.
50. Dinarello CA. 2011. Interleukin-1 in the pathogenesis and treatment of inflammatory diseases. *Blood* 117:3720-32.
51. Anand SK, Tikoo SK. 2013. Viruses as modulators of mitochondrial functions. *Adv Virol* 2013:738794.
52. Sanchez-Caballero L, Guerrero-Castillo S, Nijtmans L. 2016. Unraveling the complexity of mitochondrial complex I assembly: A dynamic process. *Biochim Biophys Acta* 1857:980-90.
53. Mokranjac D, Neupert W. 2010. The many faces of the mitochondrial TIM23 complex. *Biochim Biophys Acta* 1797:1045-54.
54. Baracca A, Chiaradonna F, Sgarbi G, Solaini G, Alberghina L, Lenaz G. 2010. Mitochondrial Complex I decrease is responsible for bioenergetic dysfunction in K-ras transformed cells. *Biochim Biophys Acta* 1797:314-23.
55. Simonnet H, Demont J, Pfeiffer K, Guenaneche L, Bouvier R, Brandt U, Schagger H, Godinot C. 2003. Mitochondrial complex I is deficient in renal oncocytomas. *Carcinogenesis* 24:1461-6.

56. Angajala A, Lim S, Phillips JB, Kim JH, Yates C, You Z, Tan M. 2018. Diverse Roles of Mitochondria in Immune Responses: Novel Insights Into Immuno-Metabolism. *Front Immunol* 9:1605.
57. Bonora E, Porcelli AM, Gasparre G, Biondi A, Ghelli A, Carelli V, Baracca A, Tallini G, Martinuzzi A, Lenaz G, Rugolo M, Romeo G. 2006. Defective oxidative phosphorylation in thyroid oncocyctic carcinoma is associated with pathogenic mitochondrial DNA mutations affecting complexes I and III. *Cancer Res* 66:6087-96.
58. Maier HJ, Britton P. 2012. Involvement of autophagy in coronavirus replication. *Viruses* 4:3440-51.
59. Kudchodkar SB, Levine B. 2009. Viruses and autophagy. *Rev Med Virol* 19:359-78.
60. Prentice E, Jerome WG, Yoshimori T, Mizushima N, Denison MR. 2004. Coronavirus replication complex formation utilizes components of cellular autophagy. *J Biol Chem* 279:10136-41.
61. Gassen NC, Niemeyer D, Muth D, Corman VM, Martinelli S, Gassen A, Hafner K, Papies J, Mosbauer K, Zellner A, Zannas AS, Herrmann A, Holsboer F, Brack-Werner R, Boshart M, Muller-Myhsok B, Drosten C, Muller MA, Rein T. 2019. SKP2 attenuates autophagy through Beclin1-ubiquitination and its inhibition reduces MERS-Coronavirus infection. *Nat Commun* 10:5770.
62. Blanco-Melo D, Nilsson-Payant BE, Liu W-C, Møller R, Panis M, Sachs D, Albrecht RA, tenOever BR. 2020. SARS-CoV-2 launches a unique transcriptional signature from in vitro, ex vivo, and in vivo systems. *bioRxiv* doi:10.1101/2020.03.24.004655:2020.03.24.004655.
63. Holownia A, Wielgat P, Rysiak E, Braszko JJ. 2016. Intracellular and Extracellular Cytokines in A549 Cells and THP1 Cells Exposed to Cigarette Smoke. *Adv Exp Med Biol* 910:39-45.
64. Lieber M, Smith B, Szakal A, Nelson-Rees W, Todaro G. 1976. A continuous tumor-cell line from a human lung carcinoma with properties of type II alveolar epithelial cells. *Int J Cancer* 17:62-70.
65. Martens K, Hellings PW, Steelant B. 2018. Calu-3 epithelial cells exhibit different immune and epithelial barrier responses from freshly isolated primary nasal epithelial cells in vitro. *Clin Transl Allergy* 8:40.
66. Shen BQ, Finkbeiner WE, Wine JJ, Mrsny RJ, Widdicombe JH. 1994. Calu-3: a human airway epithelial cell line that shows cAMP-dependent Cl⁻ secretion. *Am J Physiol* 266:L493-501.
67. Zhang X, Chu H, Wen L, Shuai H, Yang D, Wang Y, Hou Y, Zhu Z, Yuan S, Yin F, Chan JF, Yuen KY. 2020. Competing endogenous RNA network profiling reveals novel host dependency factors required for MERS-CoV propagation. *Emerg Microbes Infect* 9:733-746.
68. Travaglini KJ, Nabhan AN, Penland L, Sinha R, Gillich A, Sit RV, Chang S, Conley SD, Mori Y, Seita J, Berry GJ, Shrager JB, Metzger RJ, Kuo CS, Neff N, Weissman IL, Quake SR, Krasnow MA. 2020. A molecular cell atlas of the human lung from single cell RNA sequencing. *bioRxiv* doi:10.1101/742320:742320.

69. Ritchie ME, Phipson B, Wu D, Hu Y, Law CW, Shi W, Smyth GK. 2015. limma powers differential expression analyses for RNA-sequencing and microarray studies. *Nucleic Acids Res* 43:e47.
70. Law CW, Chen Y, Shi W, Smyth GK. 2014. voom: Precision weights unlock linear model analysis tools for RNA-seq read counts. *Genome Biol* 15:R29.
71. Yu G, Wang LG, Han Y, He QY. 2012. clusterProfiler: an R package for comparing biological themes among gene clusters. *OMICS* 16:284-7.
72. Mostafavi S, Ray D, Warde-Farley D, Grouios C, Morris Q. 2008. GeneMANIA: a real-time multiple association network integration algorithm for predicting gene function. *Genome Biol* 9 Suppl 1:S4.
73. Shannon P, Markiel A, Ozier O, Baliga NS, Wang JT, Ramage D, Amin N, Schwikowski B, Ideker T. 2003. Cytoscape: a software environment for integrated models of biomolecular interaction networks. *Genome Res* 13:2498-504.
74. Merico D, Isserlin R, Stueker O, Emili A, Bader GD. 2010. Enrichment map: a network-based method for gene-set enrichment visualization and interpretation. *PLoS One* 5:e13984.
75. Kucera M, Isserlin R, Arkhangorodsky A, Bader GD. 2016. AutoAnnotate: A Cytoscape app for summarizing networks with semantic annotations. *F1000Res* 5:1717.
76. Mehdi P. 2020. Supplemental material for Singh et al. 2020 *mBio* doi:10.6084/m9.figshare.12272351.v1.
77. Stuart T, Butler A, Hoffman P, Hafemeister C, Papalexi E, Mauck WM, 3rd, Hao Y, Stoeckius M, Smibert P, Satija R. 2019. Comprehensive Integration of Single-Cell Data. *Cell* 177:1888-1902 e21.

A

DE genes mock vs. SARS-CoV-2 (high MOI)

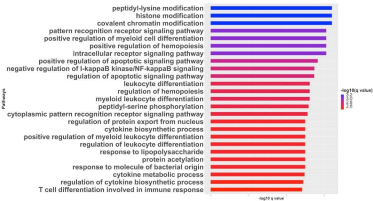
DE genes mock vs. SARS-CoV-2 (ACE2 overexpression)



899/1185 upregulated genes were further upregulated in ACE2 (oe) cells

336/669 downregulated genes were further downregulated in ACE2 (oe) cells

794 genes were inversely DE in the two comparisons

B**C**